

1-1-2010

Impacts of cloud-system resolving regional modeling on the simulation of monsoon depressions

Y. C. Wang
Purdue University

W. W. Tung
Purdue University

Follow this and additional works at: <http://docs.lib.purdue.edu/easpubs>

Repository Citation

Wang, Y. C. and Tung, W. W., "Impacts of cloud-system resolving regional modeling on the simulation of monsoon depressions" (2010). *Earth, Atmospheric, and Planetary Sciences Faculty Publications*. Paper 3.
<http://docs.lib.purdue.edu/easpubs/3>

This document has been made available through Purdue e-Pubs, a service of the Purdue University Libraries. Please contact epubs@purdue.edu for additional information.



Impacts of cloud-system resolving regional modeling on the simulation of monsoon depressions

Y.-C. Wang¹ and W.-W. Tung¹

Received 29 January 2010; revised 18 March 2010; accepted 29 March 2010; published 28 April 2010.

[1] The impacts of high-resolution (<10 km) and cloud-system-resolving regional modeling (CSRМ) on the simulation of an intense south Asian monsoon depression (MD) were examined using the WRF-ARW model. Spatial resolution in this range was necessary to realistically simulate the MD's propagation, intensity, and precipitation. Simulations were however highly sensitive to the moist convection and cloud microphysics. The best scenarios were created by the microphysics parameterization (MP) that generated the most robust post-landfall condensation associated with the MD, alone or in combination with the cumulus parameterization that triggered vigorous convection overland in the coarser setup. A sensitivity study of the MP schemes in CSRМ suggested that more sophisticated mixed-phased schemes contributed to higher simulation fidelity. Insufficient condensation and weak convection overland might induce spurious low systems over the Bay of Bengal through low-level moisture advection, which further interfered with the MD and degraded several simulations. **Citation:** Wang, Y.-C., and W.-W. Tung (2010), Impacts of cloud-system resolving regional modeling on the simulation of monsoon depressions, *Geophys. Res. Lett.*, 37, L08806, doi:10.1029/2010GL042734.

1. Introduction

[2] Monsoon depressions (MDs) are the major precipitating systems during the south Asian summer monsoon. There have been a number of observational studies on the MD occurrence, structure, and propagation [e.g., *Krishnamurti et al.*, 1975, 1976; *Douglas*, 1992]. Being significant heat sources and moisture sinks in the monsoon circulation, they play important roles in the regional energetics and hydrological cycle, and have enormous societal and economic impacts on the affected nations.

[3] A typical MD embedded in the monsoon flow has a spatial scale of a few thousand kilometers in each horizontal dimension, with rainfall concentrated in its southwest quadrant as it traverses the Indian subcontinent. Theoretical and modeling studies had suggested that cumulus heating combined with hydrodynamic instabilities may be responsible for the growth and propagation of MDs [e.g., *Krishnamurti et al.*, 1976; *Moorthi and Arakawa*, 1985; *Aravequia et al.*, 1995]. Therefore, one question to ask is how better-resolved moist convection and cloud microphysics impact the simulation of MDs. The answer is crucial for improving the NWP model's predictive utility of MDs as

well as for achieving correct regional energy balance in seasonal and climate simulations. High-resolution regional model experiments of an intense MD in AUG 2006 were performed, using the Advanced Research Weather Research and Forecast (WRF-ARW) model [*Skamarock et al.*, 2005]. The findings are reported in terms of the model's sensitivity to (1) cumulus parameterization (CP), (2) increasing grid resolution to that of the cloud-system-resolving model (CSRМ), and (3) microphysics parameterization (MP).

2. Methods and Data

2.1. Model Experiments

[4] The experiments were performed using ARW V3.0.1.1 with two-way nested domains telescoping from 27-, 9-, to the cloud-system-resolving 3-km horizontal grids, denoted as D1, D2, and D3 in Figure 1a. All domains had 35 vertical levels topped at 10 hPa. The outermost D1 covered an area over 7.3° S–40.3° N and 43.5°–120.5° E to ensure a realistic simulation of the south Asian monsoon circulation and to keep the inner domains as far away from the model's lateral boundaries as possible. The 6-hrly NCEP Final global analysis and the daily NCEP Real-Time Global Sea Surface Temperature [*Gemmill et al.*, 2007] were used as the initial and lateral boundary conditions for the D1. The integration of D1 started on JUL 25 and ended on AUG 7, 2006, allowing sufficient time for the monsoon circulation to establish before the inner domains were activated. This was achieved without data assimilation. The D2 and the D3 were initialized on JUL 31, 24 hrs before the observed MD genesis in the Bay of Bengal (BoB). The CP was turned off in the CSRМ simulations in the D3.

[5] Three experiments were performed: EXP-CP, EXP-GRID, and EXP-MP. Table 1 lists the model members in each experiment, in the format of *A-Bkm-C*. *A* indicates the choice of CP in D1 and D2, including the Kain-Fritsch (KF) [*Kain*, 2004], the Grell-Devenyi ensemble (GD) [*Grell and Devenyi*, 2002], and the Betts-Miller-Janjic (BMJ) [*Janjic*, 1994] schemes. *B* is the grid resolution of the innermost domain. *C* is the MP in all domains, including the WRF single-moment six-class microphysics (WSM6) [*Hong et al.*, 2004], the Morrison et al. (MRSN) [*Morrison et al.*, 2009], the Thompson et al. (THMP) [*Thompson et al.*, 2004], and the Kessler (KSLR) [*Kessler*, 1969] schemes. In addition, all experiments utilized the Noah land surface scheme [*Chen and Dudhia*, 2001], the Yonsei University boundary layer scheme [*Hong and Pan*, 1996], the Rapid Radiative Transfer Model scheme [*Mlawer et al.*, 1997], and the MM5 Dudhia Shortwave scheme [*Dudhia*, 1989].

2.2. Observations and Model Validation

[6] The 1.5° × 1.5° ERA-Interim reanalysis was used to validate the gross features of the simulated monsoon

¹Department of Earth and Atmospheric Sciences, Purdue University, West Lafayette, Indiana, USA.

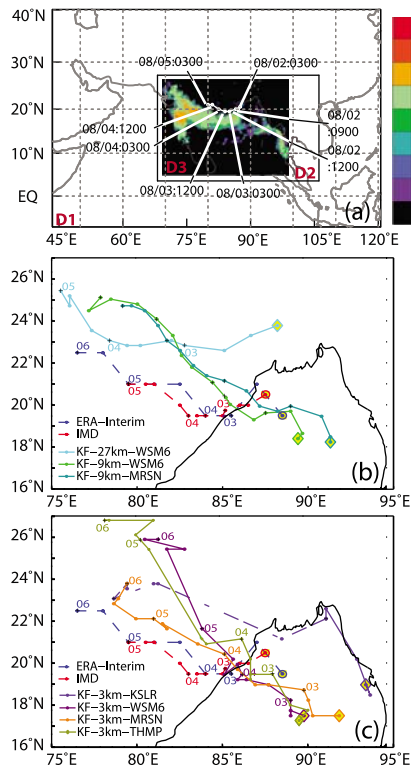


Figure 1. (a) Model domains D1, D2, and D3, with AUG 1–7, 2006, averaged TRMM rainrate mm hr^{-1} and IMD track in D3. (b and c) For 06UTC AUG 2–00UTC AUG 6, 2006, 6-hrly MD tracks from ERA-Interim, IMD, and model simulations. Yellow diamonds (simulations) and circles (IMD and ERA) denote the MD centers at 06UTC AUG 2.

circulation [Simmons *et al.*, 2007]. The TRMM 3B42 was used for rainrate validation [Simpson *et al.*, 1996; Huffman *et al.*, 1997]. It has been shown that the retrieval of ice water content (IWC) from the CloudSat Cloud Profiling Radar (CPR, [Stephens *et al.*, 2002]) may be used to preliminarily and qualitatively validate the frozen hydrometeors in CSRM simulations [Waliser *et al.*, 2009]. Thus, the IWC in CloudSat 2B-CWC-RO was utilized in such context. The mean states during AUG 1–7, 2006, are typical of the south Asian summer monsoon (see auxiliary material Figures S1 and S2).¹ Figure 1a also shows the 7-day mean of TRMM rainrate and the MD track reported by the Indian Meteorological Department [Indian Meteorological Office (IMD), 2007] in the D3. The rainfall associated with the MD extended from the western BoB to Rajasthan. The MD was first sighted as a low pressure system on AUG 1 over the northern BoB. It was strengthened into a deep depression on AUG 2 and made landfall on AUG 3. It then crossed over central India and eventually merged with the seasonal low in Pakistan.

[7] The track and intensity of the simulated MD were determined by following the minima of the mean sea-level pressure (SLP) within the depression. Figure 1 shows the observed tracks determined from the ERA-Interim using the

same method, along with the IMD report from 06UTC AUG 2 (30 hrs after MD genesis) to 00UTC AUG 6, 2006. The two observational tracks are in general agreement. Some of the simulated tracks are also shown during the same period. In addition, Figures 2a and 2b show, respectively, the time evolution of the MD intensity and the propagation speed of the MD, for the observations (left-most panels) and the simulations.

3. Results and Discussions

3.1. EXP-CP

[8] The members in EXP-CP were run in the D1-D2 nested domains (Table 1), since the simulations with D1 alone yielded far inferior results. An ensemble experiment with perturbations of the initial conditions determined that a single realization for each member was sufficient (not shown). As shown in Figure S4, the resulting rainfall distributions and MD tracks differed greatly, even though all members successfully simulated the MD's genesis and its initial tendency to propagate westward. With the KF scheme, the MD had the best overall propagation and intensity (Figures 2a, 2b, and S3), rainrate, and the asymmetric rainfall distribution (not shown). Both BMJ and GD resulted in a lack of natural variation of MD intensity (Figure 2a), unrealistic propagation (Figures 2b and S3), and weak post-landfall precipitation (not shown). BMJ triggered too much convection within the deep layer of moist air over the BoB and resulted in a spurious low almost right after the landfall of the MD, resulting in the erratic and ill-defined track in Figure S3. Despite weak precipitation, the GD run exhibited identifiable post-landfall westward propagation of the MD (Figure S3). However, it deviated to the north when the MD precipitation became disorganized spatially and a spurious low system was spun up in the BoB. The CP's ability to effectively trigger and maintain deep convection overland appeared to be the key for the inland penetration of the MD. The KF might be the most suitable scheme over land at this scale due to its design to trigger convection as long as there is convective available potential energy and its detailed updraft/downdraft mass-flux representations.

3.2. EXP-GRID

[9] The experiment was designed to assess the impact of raising the horizontal grid resolution to that of the CSRM. Based on the results in EXP-CP, KF scheme was chosen for all members. The 3-km CSRM simulations relied only on the MP scheme for subgrid effects of moist processes; therefore, two schemes (WSM6 and MRSN) were adopted to preclude dependence on a single MP. All of the simulated tracks in this experiment are plotted in Figures 1b and 1c. KF-9km-WSM6 captured the genesis, track, and propagation speed better than its 27-km counterpart. The latter

Table 1. WRF-ARW members in experiments

EXP-CP	EXP-GRID	EXP-MP
KF-9km-WSM6	KF-27km-WSM6	KF-3km-WSM6
BMJ-9km-WSM6	KF-9km-WSM6	KF-3km-MRSN
GD-9km-WSM6	KF-3km-WSM6	KF-3km-THMP
	KF-9km-MRSN	KF-3km-KSLR
	KF-3km-MRSN	

¹Auxiliary materials are available in the HTML. doi:10.1029/2010GL042734.

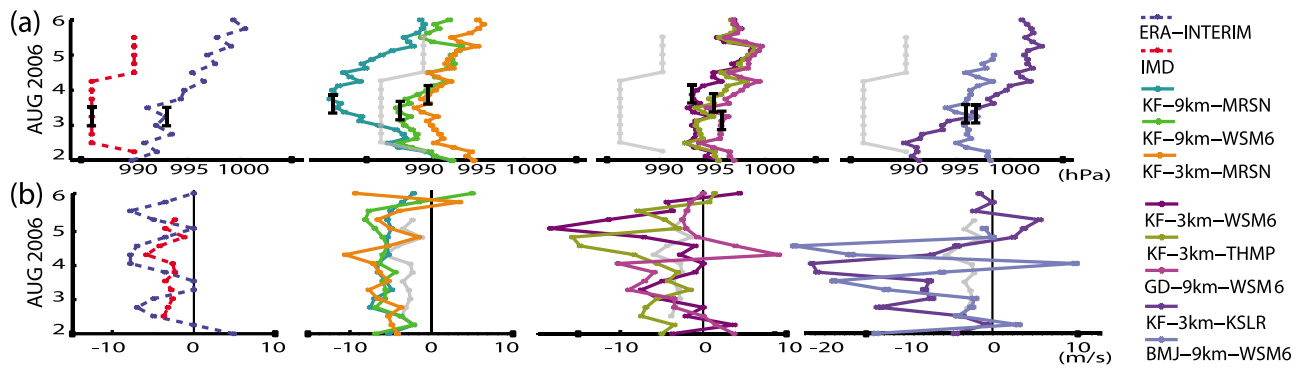


Figure 2. During AUG 2–6, 2006, the 6-hrly (a) mean SLP minima indicating the MD intensity and (b) total propagation speed (+: eastward, -: westward) of the MD. Black bars mark the approximate time of landfall; gray profiles are also IMD observations.

not only missed the MD genesis site but also placed the MD in a fast track far north. KF-9km-WSM6 and KF-9km-MRSN performed similarly in terms of the simulated tracks (Figure 1b) and propagating speeds (Figure 2b), but differed in the MD intensity (Figure 2a). They had the same northward bias in the post-landfall tracks. Both had average propagation speeds comparable to the observation ($\sim 5 \text{ m s}^{-1}$), but lacked the observed variation. The intensity difference was discernible, with the 9km MRSN run substantially over-intensifying the MD relative to the IMD analysis (Figure 2a).

[10] Degraded from KF-9km-WSM6, KF-3km-WSM6 simulated a north deviated track (Figure 1c) with much faster post-landfall propagation (Figure 2b), and lower, less varying MD intensity (Figure 2a). On the other hand, KF-3km-MRSN improved KF-9km-MRSN by better positioning the track over central India with better overall intensity. The MD also exhibited the life cycle (Figure 2a) and the variability of propagation speed such as the slow-down at landfall and speed-up afterward (Figure 2b). Further evidence of the degraded simulation from 9km- to 3km-WSM6 and improved simulation from 9km- to 3km-MRSN could be seen in the rainfall distribution (cf. TRMM in Figure S4) as well as the 850-hPa wind (cf. ERA-Interim in Figure S5). The CSRM runs generated less precipitation and weaker circulation than their 9-km counterparts. However, 3km-MRSN effectively reduced the excessive precipitation in the 9km-MRSN while the 3km-WSM6 did not produce enough.

[11] Figure S6a shows the CloudSat CPR IWC profile from 0810 to 0820UTC on AUG 3, 2006. Vertical cross-sections at approximately the same time and locations from the 3km- and 9km-MRSN runs are shown in Figures S6b and S6c to reveal the positive impact of the CSRM approach on the MD microphysics. Both simulations yielded IWC mixing ratio comparable to that of the CPR. Nevertheless, the 3km-MRSN IWC profile is tilted southward like the CPR profile. Figure S6d shows another slice through the 3km-MRSN IWC at the exact same locations as the CPR; in spite of the lower IWC mixing ratio, it suggests that the tilt is a genuine feature. This tilted structure, reflecting high clouds over the south side of MD in its outflow region and lower clouds from moist inflow over the north side of MD, is consistent with the MET-5 satellite imagery (Figure S7).

3.3. EXP-MP

[12] This experiment involved only CSRM simulations so that the model's sensitivity to the MP is addressed while limiting the influence of CP. Among the four MP schemes, i.e., WSM6, MRSN, THMP, and KSLR, the KSLR is a warm-rain scheme while the rest are mixed-phased with different degrees of complexity. The MD tracks of all members are shown in Figure 1c. As shown in Figures 1c and 2, the MD in KF-3km-KSLR originated over the far east side of the BoB, starting as a vigorous system but turning into a fast-propagating, short-lived, dry system within 48 hrs. In Figure 2 it is plotted with BMJ-9km-WSM6 as outliers among all simulations. Both KF-3km-WSM6 and KF-3km-THMP had overall weak MD with northward biased tracks, erratic post-landfall propagation speeds, and spurious lows in the BoB, which were also the characteristic shortcomings in the GD-9km-WSM6 (Figure 2). The outstanding performance of the MRSN in EXP-GRID might be attributed to its 2-moment prognostic design allowing more variability in the particle size distributions, hence the realistic number concentration distributions of hydrometeors. A preliminary analysis shows that both 3km- and 9km-MRSN runs generated a unique maximum of snow mixing ratio at $\sim 300 \text{ hPa}$ in the updraft region near the core of the MD, which might subsequently lead to more surface rainfall (not shown).

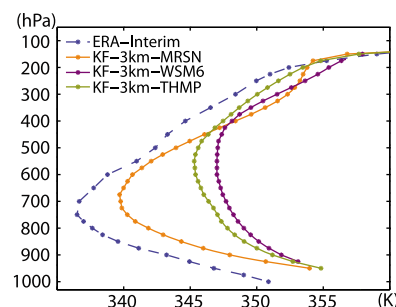


Figure 3. Averaged over the northern BoB ($17.5^\circ\text{--}22.5^\circ \text{ N}$, $87.5^\circ\text{--}92.5^\circ \text{ E}$), shown are the vertical profiles of the equivalent potential temperature (θ_e , in K) at 0000UTC AUG 5, 2006.

3.4. Spurious lows over the Bay of Bengal

[13] These were noted in KF-3km-THMP, KF-3km-WSM6 (Figure S5c), BMJ-9km-WSM6, and GD-9km-WSM6 after the MD made landfall. The circulation of the spurious lows appeared to interfere with that of the MD and inhibited the MD's inland penetration. One common feature among these runs is the diminishing rainfall in the post-landfall MD, whether it was due to ineffective convection triggering in CP or insufficient condensation in MP. Since the lower-level westerly flow from the Arabian Sea prevailed during this period (Figure S1a), the moisture excess in these runs might be advected downstream and 'recharge' the BoB to a favorable environment for the spurious lows. To confirm this, we examine the convective instability with the equivalent potential temperature (θ_e) averaged over the northern BoB (17.5–22.5° N, 87.5–92.5° E) at the time when the spurious lows formed in KF-3km-THMP and KF-3km-WSM6 (00UTC AUG 5) with Figure 3. Compared with the THMP and WSM6 runs, the KF-3km-MRSN and ERA-Interim both exhibit lower θ_e (as much as 10K) in the low- to mid-troposphere and notably shallower layers with convective instability between surface and 700 hPa; in contrast, THMP and WSM6 have potentially unstable layer extending up to 500 hPa. These differences are largely caused by the moisture since the potential temperature in the model differs no more than 3K from that of the ERA-Interim (Figure S8).

4. Conclusions

[14] Simulations of an MD event during AUG 1–7, 2006, were performed with the WRF-ARW model with two-way nested domains. Experiments were designed to understand the model's sensitivity to CP, raising grid resolution to that of the CSRM, and MP. The CP scheme's ability to effectively trigger and maintain deep convection overland appears to be essential for the inland penetration of the MD at the 9-km resolution. It is also suggested that the 9-km grids or finer are necessary to capture the MD genesis and propagation. The 3-km CSRM is a promising approach as it permits better resolved and potentially more realistic convective circulations. Fine-scale mechanisms controlling the intensity and propagation of the MD might be better simulated, if the MP can produce robust condensation overland. In the case that the MP or the CP-MP combination fails overland, spurious lows may form downstream of the low-level westerlies in the BoB, seriously limiting medium- and long-range forecasts. Sensitivity assessment of the MP schemes with CSRM runs indicates that mixed-phase microphysics may be necessary to simulate the MD and more sophisticated mixed-phased schemes may contribute to better simulations of the MD. More case studies are necessary to understand why some schemes perform better than the others. Finally, this study suggests that MPs are appropriate to be included in the physics-based high-resolution ensemble experiments and forecasts.

[15] **Acknowledgments.** The authors are grateful to C.P. Chang, H.I. Chang, R. Fovell, J.B. Gao, H. Hatwar, H.M. Hsu, T. Krishnamurti, M. Moncrieff, P. Mukhopadhyay, S. Nesbitt, W.Y. Sun, R. Trapp, M. Yanai, J.Y. Yu, and WRF-Help. Special thanks to J.L.F. Li for the CloudSat data. The computations were done at the NCAR CISL and the Purdue RCAC. The research was supported by the NSF CMMI-0826119 and 0825311.

References

- Aravequia, J., V. B. Rao, and J. Bonatti (1995), The role of moist baroclinic instability in the growth and structure of monsoon depressions, *J. Atmos. Sci.*, *52*, 4393–4409.
- Chen, F., and J. Dudhia (2001), Coupling an advanced land-surface/hydrology model with the Penn State/NCAR MM5 modeling system. Part I: Model description and implementation, *Mon. Weather Rev.*, *129*, 569–585.
- Douglas, M. W. (1992), Structure and dynamics of two monsoon depressions. Part I: Observed Structure, *Mon. Weather Rev.*, *120*, 1524–1547.
- Dudhia, J. (1989), Numerical study of convection observed during the winter monsoon experiment using a mesoscale two-dimensional model, *J. Atmos. Sci.*, *46*, 3077–3107.
- Gemmill, W., B. Katz, and X. Li (2007), Daily real-time global sea surface temperature—High resolution analysis at NOAA/NCEP, *MMAB Off. Note 260*, Natl. Cent. for Environ. Predict., Camp Springs, Md.
- Grell, G. A., and D. Devenyi (2002), A generalized approach to parameterizing convection combining ensemble and data assimilation techniques, *Geophys. Res. Lett.*, *29*(14), 1693. doi:10.1029/2002GL015311.
- Hong, S.-Y., and H.-L. Pan (1996), Nonlocal boundary layer vertical diffusion in a medium-range forecast model, *Mon. Weather Rev.*, *124*, 2322–2339.
- Hong, S.-Y., J. Dudhia, and S.-H. Chen (2004), A revised approach to ice microphysical processes for the bulk parameterization of clouds and precipitation, *Mon. Weather Rev.*, *132*, 103–120.
- Huffman, G. J., et al. (1997), The global precipitation climatology project (GPCP) combined precipitation dataset, *Bull. Am. Meteorol. Soc.*, *78*, 5–20.
- Indian Meteorological Office (2007), Cyclones and depressions over the north Indian Ocean during 2006, *Mausam*, *58*, 305–322.
- Janjic, Z. I. (1994), The step-mountain eta coordinate model: Further developments of the convection, viscous sublayer and turbulence closure schemes, *Mon. Weather Rev.*, *122*, 927–945.
- Kain, J. S. (2004), The Kain-Fritsch Convective Parameterization: An Update, *J. Appl. Meteor.*, *43*, 170–181.
- Kessler, E. (1969), *On the distribution and continuity of water substance in atmospheric circulation*, *Meteorol. Monogr.*, *32*, 84 pp., Am. Meteorol. Soc., Boston, Mass.
- Krishnamurti, T. N., M. Kanamitsu, R. Godbole, C. B. Chang, F. Carr, and J. H. Chow (1975), Study of a monsoon depression (I). Synoptic structure, *J. Meteorol. Soc. Jpn.*, *53*, 227–239.
- Krishnamurti, T. N., et al. (1976), Study of a monsoon depression (II). Dynamical structure, *J. Meteorol. Soc. Jpn.*, *54*, 208–225.
- Mlawer, E. J., S. J. Taubman, P. D. Brown, M. J. Iacono, and S. A. Clough (1997), Radiative transfer for inhomogeneous atmospheres: RRTM, a validated correlated-k model for the longwave, *J. Geophys. Res.*, *102*(D14), 16,663–16,682.
- Moorthi, S., and A. Arakawa (1985), Baroclinic instability with cumulus heating, *J. Atmos. Sci.*, *42*, 2007–2031.
- Morrison, H., G. Thompson, and V. Tatarskii (2009), Impact of cloud microphysics on the development of trailing stratiform precipitation in a simulated squall line: Comparison of one- and two-moment schemes, *Mon. Weather Rev.*, *137*, 991–1007.
- Skamarock, W. C., J. B. Klemp, J. Dudhia, D. O. Gill, D. M. Barker, W. Wang, and J. G. Powers (2005), A description of the advanced research WRF Version 2, *NCAR Tech. Note NCAR/TN-468+STR*, Natl. Cent. for Atmos. Res., Boulder, Colo.
- Simmons, A., S. Uppala, D. Dee, and S. Kobayashi (2007), ERA-Interim: New ECMWF reanalysis products from 1989 onwards, *ECMWF Newsl.*, *110*, pp. 25–35, Eur. Cent. for Medium-Range Weather Forecasts, Reading, U.K.
- Simpson, J., C. Kummerow, W. K. Tao, and R. F. Adler (1996), On the Tropical Rainfall Measuring Mission (TRMM), *Meteorol. Atmos. Phys.*, *60*, 19–36.
- Stephens, G. L., et al. (2002), The CloudSat mission and the A-Train: A new dimension of space-based observations of clouds and precipitation, *Bull. Am. Meteorol. Soc.*, *83*, 1771–1790.
- Thompson, G., R. M. Rasmussen, and K. Manning, (2004), Explicit forecasts of winter precipitation using an improved bulk microphysics scheme. Part I: Description and sensitivity analysis, *Mon. Weather Rev.*, *132*, 519–542.
- Waliser, D. E., et al. (2009), Cloud ice: A climate model challenge with signs and expectations of progress, *J. Geophys. Res.*, *114*, D00A21, doi:10.1029/2008JD010015.

W.-W. Tung and Y.-C. Wang, Department of Earth and Atmospheric Sciences, Purdue University, 550 Stadium Mall Dr., West Lafayette, IN 47907, USA. (wwtung@purdue.edu; wang201@purdue.edu)